

**Estimation of the Tangential Winds and Asymmetric Structures in Typhoon Inner Core Region Using Himawari-8**

Taiga Tsukada<sup>1</sup>, Takeshi Horinouchi<sup>1,2</sup>

<sup>1</sup>Graduate School of Environmental Science, Hokkaido University, N10W5 Sapporo, Hokkaido, 060-0810, Japan.

<sup>2</sup>Faculty of Environmental Earth Science, Hokkaido University, N10W5 Sapporo, Hokkaido, 060-0810, Japan.

**Contents of this file**

Figures S1 to S8

**Additional Supporting Information (Files uploaded separately)**

Captions for Movies S1

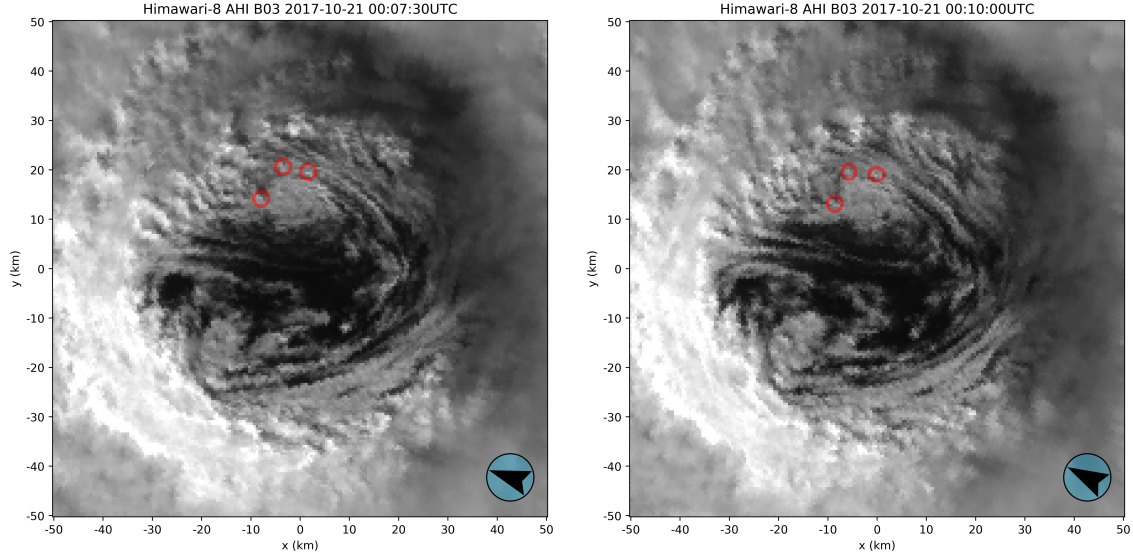


**Figure S1.** The three features around the mesovortex (MV)-1 used to derive its vorticity (red circles) shown on visible images rotated clockwise to compensate for the eye's rotation at  $r = 15$  km (see section 4.2). Left:  $(x_1^{t_0}, y_1^{t_0}) = (1.57, 19.24)$ ,  $(x_2^{t_0}, y_2^{t_0}) = (-3.6, 20.29)$ ,  $(x_3^{t_0}, y_3^{t_0}) = (-8.18, 13.74)$  at  $t_0 = 00:07:30$  UTC, 21, October. Right:  $(x_1^{t_0+\Delta t}, y_1^{t_0+\Delta t}) = (-0.26, 18.85)$ ,  $(x_2^{t_0+\Delta t}, y_2^{t_0+\Delta t}) = (-5.89, 19.37)$ ,  $(x_3^{t_0+\Delta t}, y_3^{t_0+\Delta t}) = (-8.77, 12.96)$  at  $t_0 + \Delta t = 00:10:00$  UTC, 21 in local coordinates (units: km). Black arrowhead near the lower right corner indicates the north direction.

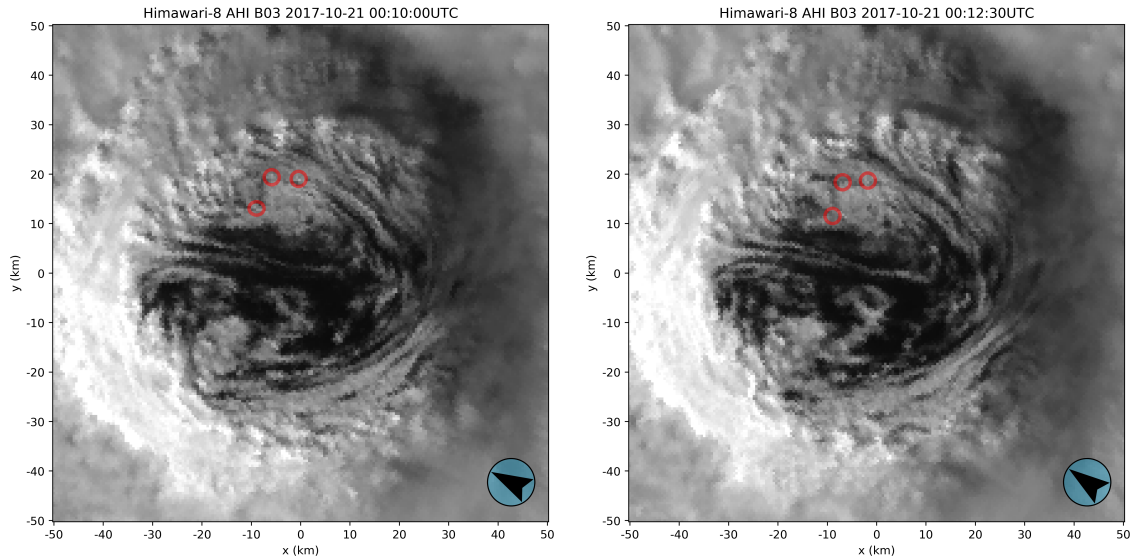


**Figure S2.** As in Fig. S1 but at different times. Left:  $(x_1^{t_0}, y_1^{t_0}) = (-0.26, -18.85)$ ,  $(x_2^{t_0}, y_2^{t_0}) = (-5.89, 19.37)$ ,  $(x_3^{t_0}, y_3^{t_0}) = (-8.77, 12.96)$  at  $t_0 = 00:10:00$  UTC, 21, October. Right:  $(x_1^{t_0+\Delta t}, y_1^{t_0+\Delta t}) = (-1.96, 18.46)$ ,  $(x_2^{t_0+\Delta t}, y_2^{t_0+\Delta t}) = (-7.07, 18.19)$ ,  $(x_3^{t_0+\Delta t}, y_3^{t_0+\Delta t}) = (-9.29, 11.39)$  at  $t_0 + \Delta t = 00:12:30$  UTC, 21.

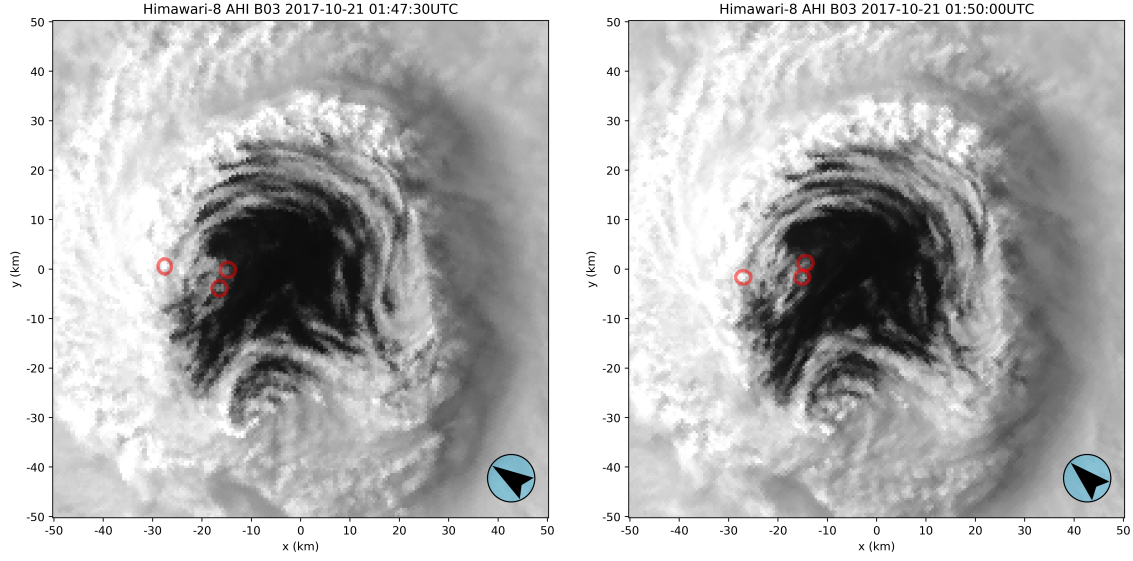


**Figure S3.** As in Fig. S1 but for MV-4 at different time. Left:  $(x_1^{t_0}, y_1^{t_0}) = (-27.36, 0.52)$ ,  $(x_2^{t_0}, y_2^{t_0}) = (-16.16, -3.93)$ ,  $(x_3^{t_0}, y_3^{t_0}) = (-14.66, -0.13)$  at  $t_0 = 01:47:30$  UTC, 21, October. Right:  $(x_1^{t_0+\Delta t}, y_1^{t_0+\Delta t}) = (-27.03, -1.70)$ ,  $(x_2^{t_0+\Delta t}, y_2^{t_0+\Delta t}) = (-14.92, -1.70)$ ,  $(x_3^{t_0+\Delta t}, y_3^{t_0+\Delta t}) = (-14.33, 1.18)$  at  $t_0 + \Delta t = 01:50:00$  UTC, 21.

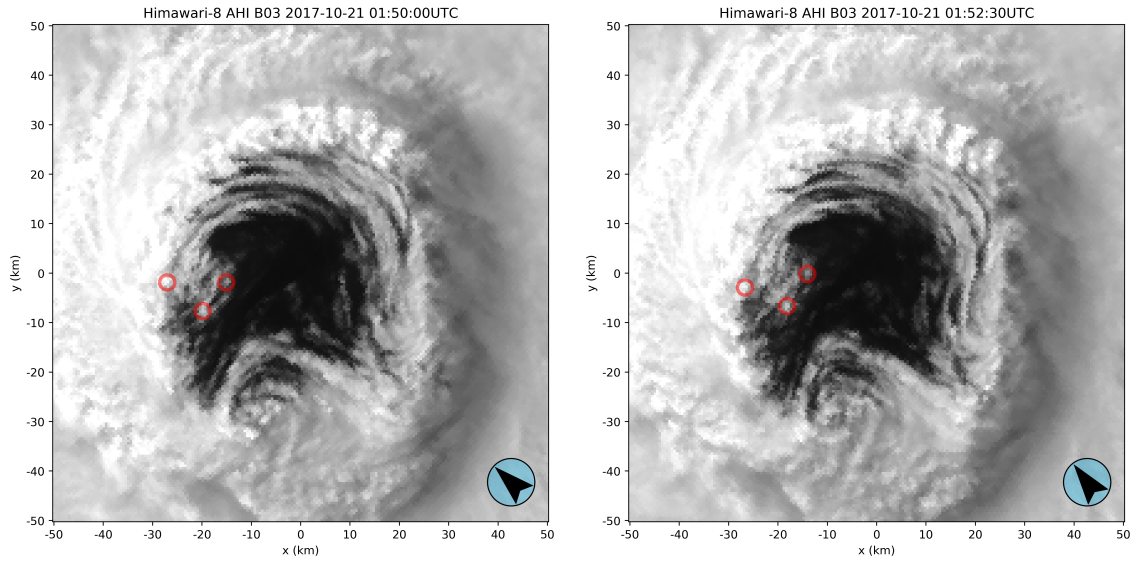


**Figure S4.** As in Fig. S1 but for MV-4 at different time. Left:  $(x_1^{t_0}, y_1^{t_0}) = (-27.03, -1.70)$ ,  $(x_2^{t_0}, y_2^{t_0}) = (-14.92, -1.70)$ ,  $(x_3^{t_0}, y_3^{t_0}) = (-19.63, -7.72)$  at  $t_0 = 01:50:00$  UTC, 21, October. Right:  $(x_1^{t_0+\Delta t}, y_1^{t_0+\Delta t}) = (-26.77, -2.62)$ ,  $(x_2^{t_0+\Delta t}, y_2^{t_0+\Delta t}) = (-14.01, 0.07)$ ,  $(x_3^{t_0+\Delta t}, y_3^{t_0+\Delta t}) = (-18.13, -6.54)$  at  $t_0 + \Delta t = 01:52:30$  UTC, 21.

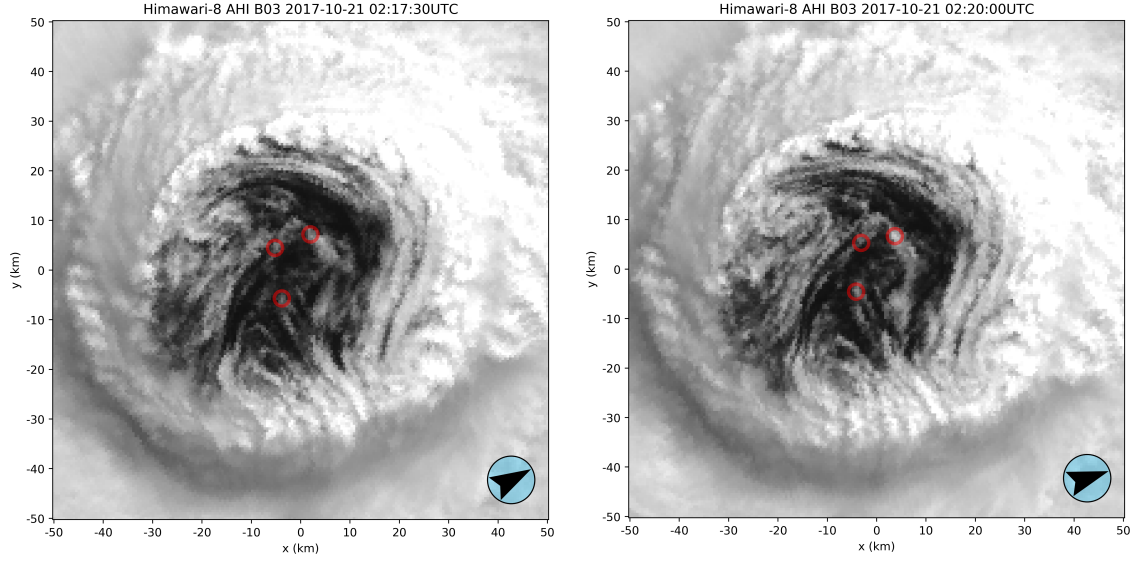


**Figure S5.** As in Fig. S1 but for MV-6 at different time. Left:  $(x_1^{t_0}, y_1^{t_0}) = (-3.73, -6.09)$ ,  $(x_2^{t_0}, y_2^{t_0}) = (2.09, 6.87)$ ,  $(x_3^{t_0}, y_3^{t_0}) = (-4.97, 4.32)$  at  $t_0 = 02:17:30$  UTC, 21, October. Right:  $(x_1^{t_0+\Delta t}, y_1^{t_0+\Delta t}) = (-4.06, -4.45)$ ,  $(x_2^{t_0+\Delta t}, y_2^{t_0+\Delta t}) = (3.47, 6.68)$ ,  $(x_3^{t_0+\Delta t}, y_3^{t_0+\Delta t}) = (-3.27, 5.37)$  at  $t_0 + \Delta t = 02:20:00$  UTC, 21.

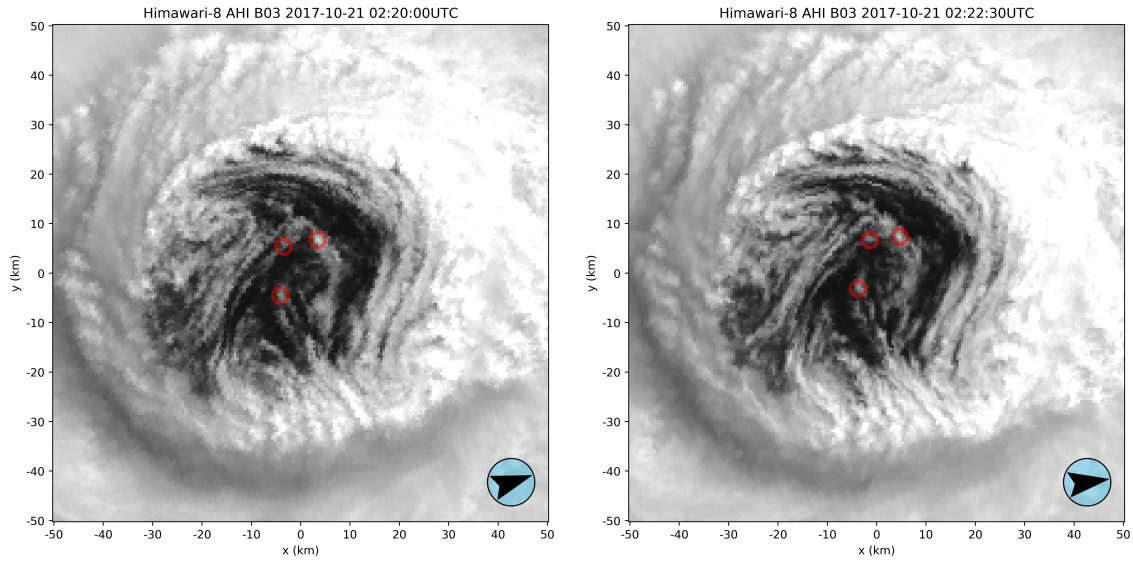


**Figure S6.** As in Fig. S1 but for MV-6 at different time. Left:  $(x_1^{t_0}, y_1^{t_0}) = (-4.06, -4.45)$ ,  $(x_2^{t_0}, y_2^{t_0}) = (3.47, 6.68)$ ,  $(x_3^{t_0}, y_3^{t_0}) = (-3.27, 5.37)$  at  $t_0 = 02:20:00$  UTC, 21, October. Right:  $(x_1^{t_0+\Delta t}, y_1^{t_0+\Delta t}) = (-3.80, -3.01)$ ,  $(x_2^{t_0+\Delta t}, y_2^{t_0+\Delta t}) = (4.65, 7.40)$ ,  $(x_3^{t_0+\Delta t}, y_3^{t_0+\Delta t}) = (-1.57, 6.87)$  at  $t_0 + \Delta t = 02:22:30$  UTC, 21.



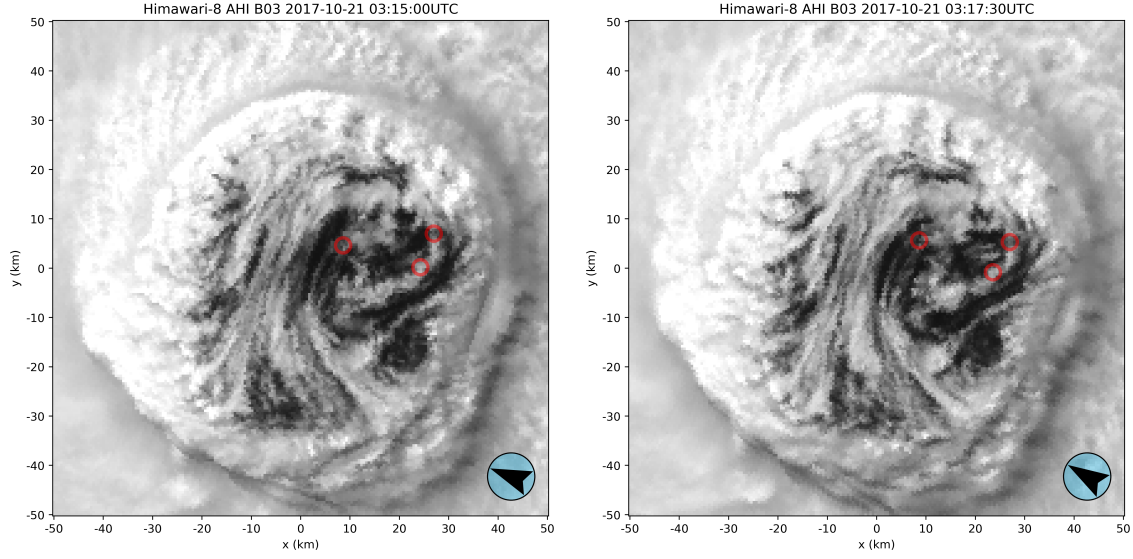


**Figure S7.** As in **Fig. S1** but for MV-6 at different time. Left:  $(x_1^{t_0}, y_1^{t_0}) = (8.44, 4.58)$ ,  $(x_2^{t_0}, y_2^{t_0}) = (24.21, 0.39)$ ,  $(x_3^{t_0}, y_3^{t_0}) = (26.83, 7.07)$  at  $t_0 = 03:15:00$  UTC, 21, October. Right:  $(x_1^{t_0+\Delta t}, y_1^{t_0+\Delta t}) = (8.57, 5.63)$ ,  $(x_2^{t_0+\Delta t}, y_2^{t_0+\Delta t}) = (23.56, -0.85)$ ,  $(x_3^{t_0+\Delta t}, y_3^{t_0+\Delta t}) = (27.16, 5.30)$  at  $t_0 + \Delta t = 03:17:30$  UTC, 21.

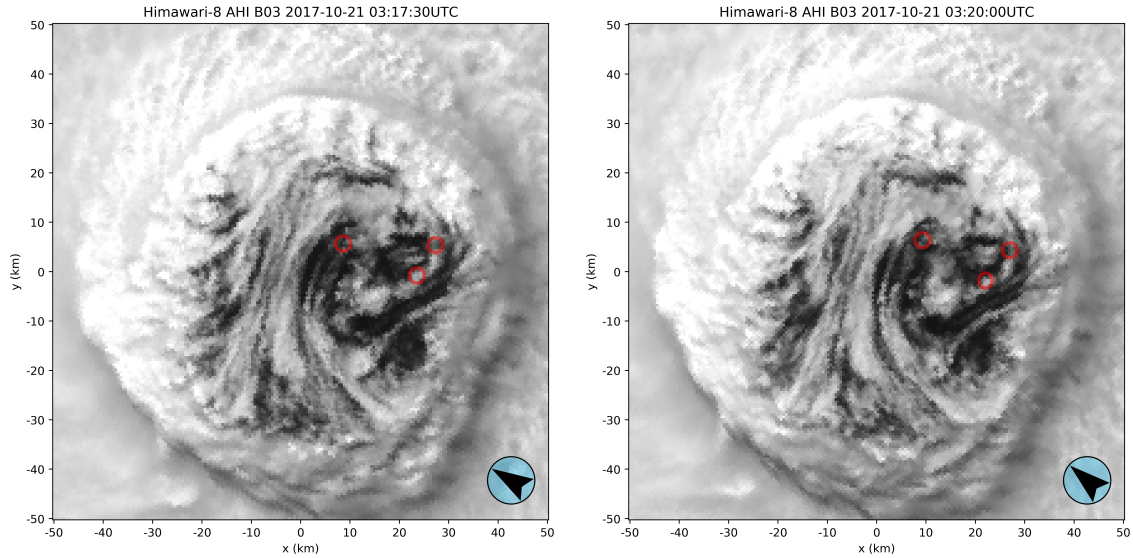


**Figure S8.** As in **Fig. S1** but for MV-6 at different time. Left:  $(x_1^{t_0}, y_1^{t_0}) = (8.57, 5.63)$ ,  $(x_2^{t_0}, y_2^{t_0}) = (23.56, -0.85)$ ,  $(x_3^{t_0}, y_3^{t_0}) = (27.16, 5.30)$  at  $t_0 = 03:17:30$  UTC, 21, October. Right:  $(x_1^{t_0+\Delta t}, y_1^{t_0+\Delta t}) = (9.42, 6.48)$ ,  $(x_2^{t_0+\Delta t}, y_2^{t_0+\Delta t}) = (22.19, -1.90)$ ,  $(x_3^{t_0+\Delta t}, y_3^{t_0+\Delta t}) = (27.16, 4.19)$  at  $t_0 + \Delta t = 03:20:00$  UTC, 21.

**Movie S1.** 2.5-minute Himawari-8 VIS images of the Typhoon Lan (2017) at  $r \leq 50$  km rotated clockwise from 22:45 UTC, 20, October to 06:45 UTC, 21, October. The images are rotated clockwise to compensate for the rotation speed of  $\sim 1.15 \times 10^{-3}$  rad/s at  $r = 15$  km (**Fig. 4**).